

Heat shock transcription factor 1-associated expression of slow myosin heavy chain in mouse soleus muscle in response to unloading with or without reloading

Shingo Yokoyama^{1,2}, Yoshitaka Ohno², Tatsuro Egawa³, Kazuyuki Yasuhara⁴, Akira Nakai⁵, Takao Sugiura⁶, Yoshinobu Ohira⁷, Toshitada Yoshioka⁸, Minoru Okita¹, Tomoki Origuchi¹, Katsumasa Goto^{2,3}

¹Department of Locomotive Rehabilitation Science, Unit of Rehabilitation Sciences, Nagasaki University Graduate School of Biomedical Sciences, Nagasaki, Japan

²Laboratory of Physiology, School of Health Science, Toyohashi SOZO University, Toyohashi, Japan

³Department of Physiology, Graduate School of Health Science, Toyohashi SOZO University, Toyohashi, Japan

⁴Department of Orthopaedic Surgery, St. Marianna University School of Medicine, Kawasaki, Japan

⁵Department of Molecular Biology, Graduate School of Medicine, Yamaguchi University, Ube, Japan

⁶Faculty of Education, Yamaguchi University, Yamaguchi, Japan

⁷Faculty and Graduate School of Health and Sports Sciences, Doshisha University,

20 Kyotanabe, Japan

21 ⁷Hirosaki Gakuin University, Hirosaki, Japan

22

23 **Short title:** HSF1 and slow myosin heavy chain

24

25 Address for correspondence;

26 Katsumasa Goto, Ph.D.

27 Department of Physiology

28 Graduate School of Health Sciences

29 Toyohashi SOZO University

30 20-1 Matsushita, Ushikawa, Toyohashi

31 Aichi 440-8511

32 Japan

33 TEL: +81 50 2017 2272

34 FAX: +81 532 55 0803

35 E-mail: gotok@sepia.ocn.ne.jp

36

Abstract

Aim: The effects of heat shock transcription factor 1 (HSF1)-deficiency on the fiber type composition and the expression level of nuclear factor of activated T cells (NFAT) family members (NFATc1, NFATc2, NFATc3, and NFATc4), phosphorylated glycogen synthase kinase 3 α (p-GSK3 α) and p-GSK3 β , microRNA-208b (miR-208b), miR-499, slow myosin heavy chain (MyHC) mRNAs (Myh7, and Myh7b) of antigravitational soleus muscle in response to unloading with or without reloading were investigated.

Methods: HSF1-null and wild-type mice were subjected to continuous 2-week hindlimb suspension followed by 2- or 4-week ambulation recovery.

Results: In wild-type mice, the relative population of slow type I fibers, the expression level of NFATc2, p-GSK3 (α and β), miR-208b, miR-499, and slow MyHC mRNAs (Myh7 and Myh7b) were all decreased with hindlimb suspension, but recovered after it. Significant interactions between train and time (the relative population of slow type I fibers; $p=0.01$, the expression level of NFATc2; $p=0.001$, p-GSK β ; $p=0.009$, miR-208b; $p=0.002$, miR-499; $p=0.04$) suggested that these responses were suppressed in HSF1-null mice.

Conclusion: HSF1 may be a molecule in the regulation of the expression of slow MyHC as well as miR-208b, miR-499, NFATc2, and p-GSK3 (α and β) in mouse soleus muscle.

56 **Key words:** heat shock transcription factor 1, myosin heavy chain, nuclear factor of

57 activated T cells, glycogen synthase kinase 3, microRNA

58

59 **Introduction**

60 Unloading, as well as inactivity, is a major cause of skeletal muscle atrophy,
61 particularly of antigravitational slow-twitch muscle, such as soleus muscle (Fitts et al., 1986,
62 Thomason et al., 1987, Ohira et al., 2006). Furthermore, a slow-to-fast transition of myosin
63 heavy chain (MyHC) isoforms is observed in unloading-associated atrophied slow soleus
64 muscle, resulting in an increase in the relative proportion of fast-twitch fibers (Diffie et al.,
65 1991, Campione et al., 1993, Haddad et al., 1998). Even though several molecules including
66 the nuclear factor of activated T cells (NFAT) family of transcription factors and noncoding
67 microRNAs (miRNAs), especially miR-208b and miR-499, has been proposed, the
68 molecular mechanisms of unloading-associated slow-to-fast transition of MyHC in
69 antigravitational soleus muscle have not yet been fully elucidated.

70 The NFAT family members, which are activated by a Ca^{2+} /calmodulin-dependent
71 protein phosphatase calcineurin, play a role as a regulatory factor for the expression of slow
72 MyHC isoforms (Naya et al., 2000) . Although the NFAT family consists of five members,
73 NFATc1, c2, c3, c4, and c5 (Rao et al., 1997), only NFATc1–4 are dephosphorylated by
74 calcineurin (Daou et al., 2013). Dephosphorylated NFAT family members translocate to the
75 nucleus, then bind DNA to transcribe the MyHC gene (Allen et al., 2001). Since the
76 inhibition of calcineurin using cyclosporine A and FK506 leads to an increase in the relative
77 proportion of fibers expressing fast MyHC (Chin et al., 1998), it is suggested that

unloading-associated slow-to-fast transition of MyHC might be attributed to suppression of the nuclear translocation of NFATs (Oishi et al., 2008). However, the up-regulation of calcineurin has been observed in unloading-associated atrophied rat soleus muscle (Sugiura et al., 2005). Therefore, calcineurin-associated dephosphorylation activity of NFATs in response to unloading could not explain a slow-to-fast transition of MyHC in atrophied skeletal muscle clearly.

On the other hand, NFATc1 among NFAT family members is most extensively studied in the regulation of slow type I MyHC expression in skeletal muscles (Kubis et al., 2002, Shen et al., 2007). Furthermore, it has been reported that NFATc1 plays a calcineurin-dependent nerve activity sensor (Tothova et al., 2006), and that four NFAT family members (NFATc1–4) play a specific role in modulating adult muscle fiber types in response to nerve activity (Calabria et al., 2009). Slow type I MyHC is expressed when all four NFAT members are actively translocated to nucleus, and fast type IIb MyHC is expressed with nuclear NFATc4 alone. These observations suggest that the expression of slow type I MyHC is highly regulated by not only the expression level but also the subcellular localization of NFAT family members.

It has been reported that the expression of NFATc2 is regulated by heat shock transcription factor 1 (HSF1), which mediates the stress response in mammalian skeletal muscle, up-regulates heat shock proteins (HSPs) by binding the heat shock element protein

97 (Lindquist, 1986), in mouse embryonic fibroblast (MEF) cells (Hayashida et al., 2010). In
98 HSF1-null MEF cells, the basal expression of NFATc2 was suppressed, compared with
99 wild-type cells. Furthermore, heat stress up-regulated NFATc2 expression in wild-type cells,
100 but not HSF1-null MEF cells (Hayashida et al., 2010). These observations strongly suggest
101 that HSF1 may regulate the expression level of MyHC though the HSF1-mediated NFATc2
102 expression in skeletal muscle cells. However, there is no evidence regarding the role of
103 HSF1 in the expression levels of not only NFAT family members, especially NFATc2, but
104 also MyHC isoforms in skeletal muscles.

105 The subcellular localization of NFAT is regulated by its phosphorylation level. Even
106 though the dephosphorylation of NFAT by calcineurin in regulation of MyHC phenotypes in
107 skeletal muscle has been extensively studied, its phosphorylation by kinases is poorly
108 understood. In the nucleus, NFAT is phosphorylated by kinases, such as glycogen synthase
109 kinase 3 (GSK3), casein kinase 1 (CK1), p38 mitogen-activated protein kinase (MAPK), and
110 c-Jun N-terminal kinase (JNK), then exported from the nucleus to the cytoplasm (Shen et al.,
111 2007). The GSK3 family of serine/threonine kinases is identified as a negative regulator of
112 glycogen synthase, and plays a role as the rate-limiting enzyme in glycogen synthesis
113 (Woodgett et al., 1982). The GSK3 family consists of 2 isoforms, α and β , which are 98%
114 identical within their kinase domains but differ substantially in their N- and C-terminal
115 sequences. It has been well known that the GSK3 β family of serine/threonine kinases, which

is downstream of phosphatidylinositol 3-kinase (PI3K)-Akt signaling pathway, is involved in glycogen synthesis and plays as a negative regulator of protein synthesis (Glass, 2003). On the other hand, it has been reported that GSK3 β phosphorylates NFATc1 in muscle nuclei (Shen et al., 2007). Therefore, GSK3 β may also play a role in the regulation of MyHC phenotypes. Although the suppression of phosphorylation level of GSK3 β and other downstreams of PI3K-Akt signaling pathway accompanying with decreased expression of slow type I MyHC during hindlimb unloading has been reported (Dupont et al., 2011), a role of GSK3 in the regulation of fiber types in skeletal muscle remains unclear. Furthermore, there is no report regarding the relationship between GSK3 β and HSF1 in skeletal muscles.

It has been also shown that increased GSK3 activity plays a role in insulin resistance (Wojtaszewski et al., 2001, Ciaraldi et al., 2007) and the activity of GSK3 α is higher than GSK3 β in rat soleus (Abaffy and Cooper, 2004). However, the responses of GSK3 α in skeletal muscles to unloading followed by reloading is still unknown.

In addition to NFAT family-mediated regulation of MyHC phenotypes, it has been also reported that miR-208b and miR-499 also play a role in the expression of slow MyHC (van Rooij et al., 2009, McCarthy et al., 2009, Gan et al., 2013). Down-regulation of both miRNAs suppresses the expression slow MyHC via the suppression of Myh7 gene, which is regulated by miR-208b, and Myh7b gene, which is regulated by miR-499 (van Rooij et al., 2009, McCarthy et al., 2009, Gan et al., 2013). However, there is no evidence regarding the

role of HSF1 in the expression levels of not only miRNAs, miR-208b and miR-499, but also Myh7 and Myh7b in skeletal muscles.

Therefore, we investigated the effects of HSF1 deficiency on the fiber type composition of mouse antigravitational soleus muscle in response to unloading with or without reloading using HSF1-null mice. Furthermore, HSF1-associated regulation of NFAT family members, GSK3, miR-208b, miR-499, and slow MyHC mRNAs (Myh7 and Myh7b) were also investigated since these molecules may be involved in the regulation of MyHC phenotypes in skeletal muscle.

Materials and Methods

Animals

All experimental procedures were carried out in accordance with the Guide for the Care and Use of Laboratory Animals as adopted and promulgated by the National Institutes of Health (Bethesda, MD, USA) and were approved by the Animal Use Committee of Toyohashi SOZO University (2007001). All treatments for animals were performed under anesthesia with *i.p.* injection of sodium pentobarbital, and all efforts were made to prevent discomfort and suffering. Male HSF1-null and wild-type (Imprinting Control Region) mice were prepared as previously described (Inouye et al., 2004). Mice at 10 to 15 weeks of age were used in this experiment ($n = 20$ for each mouse strain).

Hindlimb suspension

Hindlimb suspension was performed following the methods as described previously (Yasuhara et al., 2011). Briefly, tails of the mice were cleaned, and were loosely surrounded by adhesive tapes cross-sectionally, with a string fixed at the dorsal side of the tail, to keep the blood flow intact. The string was fastened to the roof of the cage at a height allowing the forelimbs to support the weight, yet preventing the hindlimbs from touching the floor and the sides of the cage (20 × 31 cm and 13.5 cm height). The mice could reach food and water freely by using their forelimbs. Immediately after the 2-week hindlimb suspension, ambulation recovery was allowed for 10 mice in the suspended group. During recovery, mice were housed in cages of the same size as described above. Mice in the pre-experimental control group were also housed in the cage of the same size. All mice were housed in a vivarium room with 12-h:12-h light:dark cycle and with temperature and humidity maintained at ~23°C and at ~50%, respectively. Solid food and water were provided *ad libitum*.

Sampling

Five mice of each strain were sacrificed at baseline (untreated pre-experimental control; Pre), and at 0, 2 and 4 weeks after 2-week hindlimb suspension. Soleus, but not

plantaris and gastrocnemius, muscle was used in the present study, even though some studies showed comparable atrophy in mouse soleus, plantaris, and gastrocnemius muscles following unloading (Brocca et al., 2010, Hunter and Kandarian, 2004, Mitchell and Pavlath, 2001). The soleus muscles of the suspended group were dissected from hindlimbs immediately, 2, and 4 weeks after the 2-week suspension under sodium pentobarbital anesthesia. The muscles of the pre-experimental control group were also dissected at the same respective timing, trimmed of excess fat and connective tissues, weighed, frozen in liquid nitrogen, and stored at -80°C .

Immunofluorescence fiber typing

Serial transverse cryosections (8- μm thick) of the midbelly region of the frozen right soleus muscles were cut at -20°C and mounted on slide glasses. The sections were air-dried and stained to analyze the muscle fiber typing by a standard immunohistochemical technique: Cross sections were fixed with paraformaldehyde (4%), and then post-fixed in ice-cold methanol. After blocking using a reagent (1% Roche Blocking Regent; Roche Diagnostics, Penzberg, Germany), sections were incubated with primary antibodies for slow type I MyHC (BA-F8, Developmental Studies Hybridoma Bank [DSHB], Iowa City, IA, USA) and fast type IIa MyHC (SC-71, DSHB). Sections were also incubated with secondary antibodies for anti-mouse IgG2b labeled with Alexa Flour 555 (diluted 1:200, Invitrogen,

Eugene, OR, USA) and anti-mouse IgG1 labeled with Alexa Flour 488 (diluted 1:200, Invitrogen). Images of muscle sections were obtained using a microscope (IX 81, Olympus, Tokyo, Japan) and imported into a personal computer (DP Manager Version 2.2.1.195, Olympus). The percentage of each fiber type, namely type I, IIa, and IIb/IIx, relative to total fibers in the whole cross section was calculated, based on ~100 fibers per section.

Immunoblotting analyses

The expression of NFATc1, NFATc2, NFATc3, NFATc4, phosphorylated GSK3 α (p-GSK3 α), total GSK3 α , phosphorylated GSK3 β (p-GSK3 β), total GSK3 β , and β -actin proteins were assessed by immunoblotting assay. Proximal portions of the frozen left soleus muscles were homogenized in an isolation buffer of tissue lysis reagent (CellLytic-MT, Sigma-Aldrich, ST. Louis, MO, USA) with 1% (v/v) Protease/Phosphatase Inhibitor Cocktail (#5872, Cell Signaling Technology Inc., Danvers, MA, USA) with a glass homogenizer. The homogenates were centrifuged at $15,000 \times g$ (4°C for 15 min), and the supernatant was collected. A part of the supernatant was solubilized in SDS sample buffer (30% v/v glycerol, 10% v/v 2-mercaptoethanol, 2.3% w/v SDS, 62.5 mM Tris-HCl, 0.05% w/v bromophenol blue, pH 6.8) at a concentration of 0.5 mg of protein ml⁻¹ and was incubated at 95°C for 5 min. SDS- PAGE was carried out on 8 or 12.5% polyacrylamide containing 0.5% SDS at a constant current of 20 mA for 120 min as described previously (Yasuhara et al., 2011,

Nishizawa et al., 2013, Koya et al., 2013). Equal amounts of protein (10 µg) were loaded on each gel. Molecular weight markers (#161-0374, Bio-Rad, Hercules, CA, USA) were applied to both sides of 14 lanes as the internal controls for the transfer process and electrophoresis.

Following SDS-PAGE, proteins were transferred to polyvinylidene fluoride membrane (0.2-µm pore size, Bio-Rad) at a constant voltage of 100 V for 60 min at 4°C. The membranes were blocked for 1 h at room temperature in a blocking buffer: 5% (w/v) skim milk with 0.1% Tween 20 in Tris-buffered saline (TBS) at pH 7.5. The membranes were then incubated for 1 h with polyclonal antibodies for NFATc1 (sc-13033, Santa Cruz Biotechnology, Dallas, TX, USA), NFATc2 (#4386, Cell Signaling Technology), NFATc3 (sc-8321, Santa Cruz Biotechnology), NFATc4 (ab62613, Abcam, Cambridge, UK), p-GSK3α (#9316, Cell Signaling Technology), total GSK3α (#4337, Cell Signaling Technology), p-GSK3β (#5558, Cell Signaling Technology), total GSK3β (#9315, Cell Signaling Technology), β-actin (#4967, Cell Signaling Technology), and then reacted with a secondary antibodies (goat anti-rabbit or horse anti-mouse IgG horseradish peroxidase-linked antibody, Cell Signaling Technology). After the final wash protein bands were visualized by chemiluminescence (ECL Select Western blotting kit; GE Healthcare, UK) and signal density was measured by Light-Capture (AE-6971) using CS Analyzer version 2.08b (ATTO Corporation, Tokyo, Japan). Each sample was investigated in duplicate, at least, to ensure that results were not influenced by loading errors. The densities of β-actin

were evaluated to verify equal loading. Standard curves were constructed during the preliminary experiments to ensure linearity.

Real-time reverse transcription-polymerase chain reaction (Real-time RT-PCR)

Real-time RT-PCR analysis was performed, as was described previously (Egawa et al., 2014). Briefly, total RNA was extracted from the distal portions of the muscles using the miRNeasy Mini kit (Qiagen, Hilden, Germany) according to the manufacturer's protocol. For the analyses of Myh7 and Myh7b, the RNA was reverse-transcribed to cDNA using PrimeScript RT Master Mix (Takara Bio, Otsu, Japan). Real-time RT-PCR was then performed on the cDNA (Thermal Cycler Dice Real Time System IIMRQ, Takara Bio) using Takara SYBR Premix Ex Taq II (Takara Bio). For the analyses of miR-208b and miR-499 RNA, cDNA was reverse-transcribed using a Mir-XTM 198 miRNA First Strand Synthesis Kit (Clontech Laboratories, CA, USA), and then real-time RT-PCR performed using a Mir-XTM 200 miRNA qRT-PCR SYBR Kit (Clontech Laboratories). The real-time cycle conditions were 95°C for 30 s followed by 40 cycles at 95°C for 5 s and at 60°C for 30 s for mRNA.

The relative fold change of expression was calculated by the comparative threshold cycle (CT) method using Takara Thermal Cycler Dice Real Time System Software Ver. 4.00 (Takara Bio). To normalize for the amount of total RNA present in each reaction, GAPDH

for Myh7 and Myh7b, and U6 for miR208b and miR499 were used as internal standards.

Primers were designed by using the Takara Bio Perfect Real Time Support System (Takara

Bio). The following primers were used: Myh7,

5'-GCCAACTATGCTGGAGCTGATGCCC-3' (forward) and

5'-GGTGCGTGGAGCGCAAGTTTGTCTATAAG-3' (reverse); Myh7b,

5'-ATGCAGGACCTGGTGGACA-3' (forward) and

5'-CTTGCGGTACTTAGCCAGGTTG-3' (reverse); GAPDH,

5'-TGTGTCCGTCGTGGATCTGA-3' (forward) and

5'-TTGCTGTTGAAGTCGCAGGAG-3' (reverse); miR-208b,

5'-ACAAACCTTTTGTTCGTCTT-3' (forward); miR-499, 5'-ACATCACTGCAAGTCTT-3'

(forward). The U6 primer and reverse primers for miRNAs were provided with the kit.

Statistical analyses

All values were expressed as means \pm SEM. Statistical significance was analyzed by

using two-way (strain and time) ANOVA followed by Tukey–Kramer post hoc test. The

significance level was defined as $p < 0.05$.

Results

Body weight and soleus muscle wet weight

Changes in body weight, absolute muscle wet weight, and muscle weight relative to body weight of HSF1-null and wild-type mice are shown in Figure 1. There was a significant difference in body weight during the experimental period between HSF1-null and wild-type mice ($p=0.00002$, strain effect). A significant time effect was also observed ($p=0.003$).

There was a significant time effect in absolute muscle wet weight ($p=0.002$) and muscle weight relative to body weight ($p=0.02$) during the experimental period. Significant decreases in soleus muscle weight in both types of mice were observed following 2-week hindlimb suspension ($p<0.05$). In wild-type mice, soleus muscle weight increased by 67% after 2-week recovery following the suspension. However, soleus muscle weight of HSF1-null mice only increased by 40% after 2-week recovery.

Fiber type composition of soleus muscle

First of all, we investigated the effects of HSF1 deficiency on the fiber type composition. Adult mouse soleus muscles have major populations of slow type I and fast type IIa MyHC, with a minor population of fibers expressing fast type IIb or IIx MyHC (Sandona et al., 2012). To determine the fiber type composition of soleus muscles serial muscle cryosections were stained with monoclonal antibodies specific for slow type I and fast IIa MyHC subtypes. Type IIb/IIx fibers were identified by the absence of reactivity to two antibodies (Figure 2A). Therefore, we did not distinguish between type IIb and IIx

287 MyHC.

288 Figure 2B shows the responses of the fiber type composition of soleus muscle from
 289 HSF1-null and wild-type mice to hindlimb unloading with or without reloading. There was a
 290 significant interaction in the response of the relative populations of type I ($p=0.01$) and IIa
 291 ($p=0.03$) fiber to 2-week hindlimb suspension followed by 4-week ambulation recovery
 292 between strain and time during the experimental period. In wild-type mice, the relative
 293 populations of type I, IIa, and IIb/x fibers of control soleus muscle were ~50%, ~39%, and
 294 ~10%, respectively. The relative populations (~38%) of type I control soleus muscle in
 295 HSF1-null mice was significantly lower than that in wild-type mice ($p=0.04$). However, the
 296 IIb/x fibers of control soleus muscle in HSF1-null mice were significantly higher than those
 297 in wild-type mice ($p=0.04$).

298 In wild-type mice, a significant decrease in the relative population of type I fibers
 299 ($p=0.003$) and a significant increase in the population of type IIa fibers ($p=0.001$) were
 300 observed immediately after the hindlimb suspension and after 2-weeks of recovery following
 301 the suspension, compared with the pre-experimental controls. However, no significant
 302 changes in fiber type composition of soleus muscle in HSF1-null mice were observed during
 303 the experimental period.

304

305 *Expressions of NFAT isoforms*

Since small population of type I fibers in HSF1-null mice may be attributed to the lower expression levels of NFAT family members compared with wild-type mice, we investigated the effects of HSF1 deficiency on the basal expression level of NFAT family members, NFATc1, c2, c3, and c4 (Figure 3). Basal expression level of NFATc2 in HSF1-null mice was significantly lower ~81% than that in wild-type mice ($p=0.0003$). However, there was no difference between HSF1-null and wild-type mice in the basal expression levels of NFATc1, c3, and c4.

Furthermore, we also investigated the changes in the expression levels of NFAT family members in response to hindlimb suspension followed by ambulation recovery (Figure 3). There was a significant time effect in expressions of NFATc1 during the experimental period ($p=0.0008$). A significant increase of NFATc1 expression in both types of mice was observed following 2-weeks of hindlimb suspension ($p<0.05$). The expression level of NFATc1 in both types of mice was then decreased during the recovery period.

There was a significant interaction between strain and time in the expressions of NFATc2 following 2-week hindlimb suspension and ambulation recovery ($p=0.001$). In wild-type mice, a significant decrease in the expression of NFATc2 was observed following 2-week hindlimb suspension ($p=0.006$) and a 4-week recovery ($p=0.0002$), compared with the values at the pre-experimental control. The expression level of NFATc2 in wild-type mice after 2 weeks of recovery (R2) was significantly higher than that of immediately after

the suspension (R0). However, there was no significant change in NFATc2 expression in soleus muscle in HSF1-null mice in response to suspension followed by ambulatory recovery. No significant change in the expression levels of NFATc3 and c4 during the experimental period was observed in either mouse strain.

Phosphorylation level of GSK3 α and GSK3 β

Since GSK3 β phosphorylates NFATc1 in muscle nuclei (Shen et al., 2007). We hypothesized that higher activity of GSK3 may be attributed to the small population of type I fibers in HSF1-null mice, in part. The basal phosphorylation levels of GSK3 α and GSK3 β in soleus muscles in wild-type mice were significantly lower than those in HSF1-null mice ($p=0.0006$ and $p=0.00002$, respectively, Figure 4). GSK3 α and GSK3 β activities in soleus muscle in HSF1-null mice might be significantly higher than those in wild-type mice, because GSK3 activity is negatively regulated by its phosphorylation.

Figure 4 also shows the changes in the phosphorylation levels of GSK3 α and GSK3 β in soleus muscles in response to hindlimb suspension followed by ambulation recovery. There was a significant difference in the phosphorylation level of GSK3 α during the experimental period between HSF1-null and wild-type mice ($p=0.0003$, strain effect). A significant time effect was also observed ($p=0.02$). There was a significant interaction between strain and time in the phosphorylation level of GSK3 β following hindlimb

suspension and ambulation recovery ($p=0.009$).

In wild-type mice, a large decrease in the phosphorylation levels of GSK3 α and GSK3 β was observed following 2-week hindlimb suspension. The suppression of both enzymes was stable during the 4-week recovery period. The phosphorylation level of GSK3 β in pre-experimental controls was significantly higher than that immediately after hindlimb suspension (R0), 2-week recovery (R2) and 4-week recovery (R4) ($p=0.0001$, $p=0.01$ and $p=0.00001$, respectively). However, there was no significant change in the phosphorylation level of GSK3 β in HSF1-null mice in response to hindlimb unloading followed by 4-weeks of recovery.

Expression levels of miRNAs

We also investigated the effects of HSF1 deficiency on the expression level of miR-208b and miR-499, which play a crucial role in regulation of slow type I MyHC expression. The basal expression levels of miR-208b and miR-499 in control soleus muscles in HSF1-null mice were significantly lower than those in wild-type mice ($p=0.0007$ and $p=0.03$, respectively, Figure 5).

Changes in the expressions of miRNAs (miR-208b and miR-499) are shown in Figure 5. There was a significant interaction between strain and time in the expressions of miR-208b ($p=0.002$) and miR-499 ($p=0.04$) following hindlimb suspension followed by

ambulation recovery. The expression levels of both miRNAs in HSF1-null mice were stable during the experimental period. However, in wild-type mice, significant decreases in the expression levels of miR-208b and miR-499 were observed in response to 2-week hindlimb suspension ($p < 0.05$), then showing a trend towards recovery to control levels. There were significant differences between HSF1-null and wild-type mice in the expression levels of miR-208b after 2- ($p = 0.005$) and 4-week recoveries ($p = 0.0004$).

Expression levels of slow MyHC mRNAs

We also investigated whether lower expression level of miR-208b and miR-499 in HSF1-null mice was accompanied by the lower expression levels of slow MyHC mRNAs, Myh7 and Myh7b, since miR-208b and miR-499 play as post-transcriptional regulators of Myh7 and Myh7b, respectively (van Rooij et al., 2009, McCarthy et al., 2009, Gan et al., 2013). The basal expression levels of Myh7 and Myh7b mRNAs in control soleus muscle in HSF1-null mice were lower than those in wild-type mice (Figure 6).

Changes in the expressions of Myh7 and Myh7b in response to hindlimb suspension followed by reloading are shown in Figure 6. There was a significant difference in the expressions of Myh7 ($p = 0.03$) and Myh7b ($p = 0.009$) mRNAs during the experimental period between HSF1-null and wild-type mice (strain effect). The expression level of both mRNAs in wild-type mice and Myh7 mRNA in HSF1-null mice showed a trend towards a decrease in

response to hindlimb suspension, then recovery to control levels. Myh7 mRNA in wild-type and HSF-null mice were decreased by 75% and 68% following hindlimb suspension, respectively. However, the expression level of Myh7b mRNA in HSF1-null mice was stable during the experimental period.

Discussion

The present study showed that the relative population of slow type I fibers, the expression level of NFATc2, p-GSK3 α/β , miR-208b, miR-499, and slow MyHC mRNAs (Myh7 and Myh7b) in mouse soleus muscle were suppressed by the absence of the HSF1 gene. In wild-type mice, the expression levels of these molecules decreased immediately after hindlimb suspension, then recovered to control levels. Unloading-associated decrease in the population of slow type fiber as well as the expression level of NFATc2, miR-208b, miR-499, p-GSK3 α/β , and Myh7b mRNA in mouse soleus muscle was attenuated by HSF1 deficiency.

Effects of HSF1 deficiency on the expression level of slow MyHC mRNAs and the fiber type composition in response to unloading with or without reloading

In the present study, there was no significant difference between wild-type and HSF1-null mice in the degree of muscle atrophy induced by unloading. However, the

recovery of atrophied soleus muscle mass was partially retarded by the absence of HSF1 gene. These results are consistent with a previous study (Yasuhara et al., 2011).

This study revealed a low basal expression level of slow MyHC mRNAs (Myh7 and Myh7b), the population of slow fibers expressing type I MyHC, and a high basal population of fast fibers expressing type IIb/x MyHC in soleus muscle in HSF1-null mice, compared with wild-type mice. This is the first report showing the effects of HSF1 deficiency on slow MyHC and fiber type composition in mouse soleus muscle. Furthermore, unloading-associated slow-to-fast transition of fiber types in soleus muscle was observed in wild-type mice, but not in HSF1-null mice. This transition was accompanied with the decline of Myh7 mRNA expression level. There are many reports showing that gravitational unloading increases in the population of fast fibers expressing type IIa and/or IIx MyHC in mammalian antigravitational soleus muscle (Caiozzo et al., 1997, Thomason and Booth, 1990, Diffie et al., 1991, Campione et al., 1993, Haddad et al., 1998). However, this is the first study reporting the responses of the expression levels of slow MyHC mRNAs and the fiber type composition to hindlimb unloading with or without reloading in HSF1-null mice.

The present study demonstrated that the expression level of both Myh7 and Myh7b mRNAs in wild-type mice showed a trend towards a decrease in response to hindlimb suspension, then recovery to control levels. This trend was similar with the composition of slow type I fiber population in response to unloading followed by reloading. However, the

magnitude of these changes in mRNAs are larger than that in type I MyHC. Similar tendency was also observed in the basal expression level of Myh7 and Myh7b mRNAs. Basal expression level of mRNAs in HSF1-null mice was lower ~71% and ~35% than wild-type mice. Similar phenomena have been reported by several researchers (Lodka et al., 2015, Reilly et al., 2000). Unknown mechanisms may be involved in the post-translational regulation of MyHC. Some researchers reported that the number of hybrid fibers may increase in unloaded soleus muscle. Although, in the present study, we also counted the number of hybrid fibers, it was less than 2% in all groups. Therefore, we have no clear explanation about this phenomena at present.

Possible mechanism(s) of miRNAs in the basal expression level of slow MyHC

In relation to a possible role of miRNAs-dependent mechanisms in HSF1 deficiency-associated suppression of slow type I MyHC, we investigated the expression level of miR-208b and miR-499 in soleus muscle. This revealed a low basal expression level of miR-208b and miR-499 of soleus muscle in HSF1-null mice, compared with wild-type mice. This is the first study investigating the expression levels of miR-208b and miR-499 in the skeletal muscle of HSF1-null mice. Although HSF1 regulates various miRNAs (Feng et al., 2014, Das and Bhattacharyya, 2014, Li et al., 2014), there has been no previous report showing HSF1-dependent regulation of miR-499 and 208b.

It has been reported that the expression level of slow MyHC mRNAs (Myh7 and Myh7b) are highly regulated by miR-208b and miR-499, respectively (Gan et al., 2013, McCarthy et al., 2009, van Rooij et al., 2009). In the present study, the basal expression level of Myh7 and Myh7b mRNAs in HSF1-null was significantly lower than that in wild-type mice. Even though we have no clear explanation for the low basal expression levels of miR-208b and miR-499, their expression levels could explain the population of slow fibers expressing type I MyHC.

Possible mechanism(s) of GSK3/NFAT-dependent signals in the basal expression level of slow MyHC

To investigate a possible role of GSK3/NFAT-dependent mechanism(s) in HSF1 deficiency-associated suppression of slow type I MyHC, we evaluated the expression level of NFAT family members and p-GSK3 α/β in soleus muscles. We found low basal expression levels of NFATc2 and p-GSK3 β in soleus muscle in HSF1-null mice, compared with wild-type mice. Since a previous study reported HSF1-dependent up-regulation of NFATc2 in MEF cells (Hayashida et al., 2010), HSF1 may play a role in the up-regulation of NFATc2 in soleus muscle cells. It has been reported that the knockdown of NFATc2 and NFATc4 induced the suppression of type I MyHC in human skeletal muscle myoblasts (Yamaguchi et al., 2013). Although in the present study the expression level of NFATc2 in soleus mouse

muscle was suppressed by HSF1 deficiency, the expression levels of NFATc4 in wild-type and HSF1-null mice were comparable. Therefore, the basal population of slow type I fibers in mouse soleus muscle may be regulated by the expression level of NFATc2, but not NFATc4.

This is the first study investigating the expression level of GSK3 (GSK3 α and GSK3 β) in the skeletal muscle of HSF1-null mice. Although a molecular mechanism of HSF1-deficiency-associated suppression of GSK3 remains unclear, low expression levels of p-GSK3, which means high activity of GSK3, might stimulate the export of nuclear NFAT (Neal and Clipstone, 2001, Beals et al., 1997), and depress the content of NFATs in the nucleus. It has been reported that GSK3 plays a role in the up-regulation of slow MyHC2 in chicken skeletal muscle fiber (Jiang et al., 2006). A GSK3-dependent mechanism might also play a role in modulating the population of slow fibers in skeletal muscle.

Possible mechanism(s) of miRNAs- and GSK3/NFAT-dependent signals in the expression levels of slow MyHC in response to unloading with or without reloading

In this study, the responses of miRNAs (miR-208b and miR-499), NFATc2, and p-GSK3 (α and β), to unloading with or without reloading in HSF1-null mice were different from those in wild-type mice. In wild-type mice, the expression levels of miR-208b, miR-499, NFATc2, and p-GSK3 (α and β) decreased in response to unloading, and miR-208b,

477 miR-499, and NFATc2, but not p-GSK3 (α and β), transiently increased during recovery.
 478 Previous studies have also showed unloading-associated suppression of miR-208b and
 479 miR-499 in rat soleus muscle (McCarthy et al., 2009). Regarding the expression level of
 480 p-GSK3 β in response to unloading and reloading, the responses to unloading were
 481 controversial among the previous studies. In rat soleus muscle, p-GSK3 β expression was
 482 decreased by 2-week hindlimb suspension (McCarthy et al., 2009). This result was
 483 consistent with that of the present study. There is, however, a report that p-GSK3 β
 484 expression in mouse soleus muscle exhibited no change following 2-week hindlimb
 485 unloading (van der Velden et al., 2007, White et al., 2015). Furthermore, 10-day hindlimb
 486 immobilization had no effect on the expression level of p-GSK3 β in rat soleus muscle
 487 (Childs et al., 2003). On the other hand, reloading-associated up-regulation of p-GSK3 β was
 488 observed in unloaded soleus muscle of rat and mouse (Dupont et al., 2011, van der Velden et
 489 al., 2007). There is no report regarding the effects of hindlimb unloading and reloading on
 490 the expression of p-GSK3 α .

491 Expression of these molecules in HSF1-null mice was stable during hindlimb
 492 unloading with or without reloading. This is the first investigation showing the responses of
 493 the expression levels of miR-208b, miR-499, NFATc2, and p-GSK3 (α and β) in soleus
 494 muscle in HSF1- null mice. Taken together with a roles of miRNAs-, NFATc2-, and
 495 GSK3-dependent mechanisms in the modulation of slow type I MyHC, the

unloading-associated decrease in the population of slow fibers might be attributed to low expression levels of miR-208b, miR-499, NFATc2, and p-GSK3. Therefore, miRNAs-, NFATc2-, and GSK3-dependent mechanisms might play a crucial role in the unloading-associated slow-to-fast transition of fibers types in soleus muscle. However, reloading-associated expression of MyHC in atrophied soleus muscle could not be explained by changes in the expression levels of these molecules, since the activities of NFATc2 and pGSK3 in mechanisms of MyHC regulations depend mostly on phosphorylation and translocation to and out of myonuclei. Furthermore, the involvement of FOXO transcription factor 1, one of the negative regulators of PI3K/Akt signaling pathway, in slow type MyHC regulation (Sandri et al., 2004, Kamei et al., 2004) has been proposed. MyHC phenotypes in response to reloading on atrophied soleus muscle might be regulated by other, currently unknown, mechanism(s).

In conclusion, the basal expression of slow MyHC mRNAs, Myh7 and Myh7b, and the population of slow type I fibers in mouse soleus muscle was suppressed by the absence of HSF1. Furthermore, unloading-associated decline of Myh7b mRNA expression and the number of slow type fiber in mouse soleus muscle were attenuated by HSF1 deficiency. These observations suggests that HSF1 may be a molecule in the regulation of the expression of slow MyHC as well as miR-208b, miR-499, NFATc2, and p-GSK3 (α and β) in mouse soleus muscle.

515 **Acknowledgments**

516 The authors thank Dr. L. L. Tang of the Department of Physiology, Graduate School of
517 Health Sciences, and Toyohashi SOZO University for his technical assistance.

518

519 **Conflicts of interest**

520 The authors state that there are no conflicts of interest.

521

522 **Grants**

523 This study was supported, in part, by Grants-in-Aid for Challenging Exploratory
524 Research (26560372, KG), and Grants-in-Aid for Scientific Research (C, 26350818, TY)
525 from the Japan Society for the Promotion of Science, the Uehara Memorial Foundation (KG),
526 the Naito Foundation (KG), and Graduate School of Health Sciences, Toyohashi SOZO
527 University (KG).

528

References

- Abaffy, T. & Cooper, G. J. 2004. GSK3 involvement in amylin signaling in isolated rat soleus muscle. *Peptides*, **25**, 2119-25.
- Allen, D. L., Sartorius, C. A., Sycuro, L. K. & Leinwand, L. A. 2001. Different pathways regulate expression of the skeletal myosin heavy chain genes. *J Biol Chem*, **276**, 43524-33.
- Beals, C. R., Sheridan, C. M., Turck, C. W., Gardner, P. & Crabtree, G. R. 1997. Nuclear export of NF-ATc enhanced by glycogen synthase kinase-3. *Science*, **275**, 1930-4.
- Brocca, L., Pellegrino, M. A., Desaphy, J. F., Pierno, S., Camerino, D. C. & Bottinelli, R. 2010. Is oxidative stress a cause or consequence of disuse muscle atrophy in mice? A proteomic approach in hindlimb-unloaded mice. *Exp Physiol*, **95**, 331-50.
- Caiozzo, V. J., Baker, M. J., McCue, S. A. & Baldwin, K. M. 1997. Single-fiber and whole muscle analyses of MHC isoform plasticity: interaction between T3 and unloading. *Am J Physiol*, **273**, C944-52.
- Calabria, E., Ciciliot, S., Moretti, I., Garcia, M., Picard, A., Dyar, K. A., Pallafacchina, G., Tothova, J., Schiaffino, S. & Murgia, M. 2009. NFAT isoforms control activity-dependent muscle fiber type specification. *Proc Natl Acad Sci U S A*, **106**, 13335-40.
- Campione, M., Ausoni, S., Guezennec, C. Y. & Schiaffino, S. 1993. Myosin and troponin

- 548 changes in rat soleus muscle after hindlimb suspension. *J Appl Physiol*, **74**, 1156-60.
- 549 Childs, T. E., Spangenburg, E. E., Vyas, D. R. & Booth, F. W. 2003. Temporal alterations in
550 protein signaling cascades during recovery from muscle atrophy. *American Journal*
551 *of Physiology: Cell Physiology*, **285**, C391-8.
- 552 Chin, E. R., Olson, E. N., Richardson, J. A., Yang, Q., Humphries, C., Shelton, J. M., Wu, H.,
553 Zhu, W., Bassel-Duby, R. & Williams, R. S. 1998. A calcineurin-dependent
554 transcriptional pathway controls skeletal muscle fiber type. *Genes Dev*, **12**, 2499-509.
- 555 Ciaraldi, T. P., Nikoulina, S. E., Bandukwala, R. A., Carter, L. & Henry, R. R. 2007. Role of
556 glycogen synthase kinase-3 alpha in insulin action in cultured human skeletal muscle
557 cells. *Endocrinology*, **148**, 4393-9.
- 558 Daou, N., Lecolle, S., Lefebvre, S., della Gaspera, B., Charbonnier, F., Chanoine, C. &
559 Armand, A. S. 2013. A new role for the calcineurin/NFAT pathway in neonatal
560 myosin heavy chain expression via the NFATc2/MyoD complex during mouse
561 myogenesis. *Development*, **140**, 4914-25.
- 562 Das, S. & Bhattacharyya, N. P. 2014. Heat shock factor 1 regulates hsa-miR-432 expression
563 in human cervical cancer cell line. *Biochem Biophys Res Commun*, **453**, 461-6.
- 564 Diffie, G. M., Haddad, F., Herrick, R. E. & Baldwin, K. M. 1991. Control of myosin heavy
565 chain expression: interaction of hypothyroidism and hindlimb suspension. *Am J*
566 *Physiol*, **261**, C1099-106.

- 567 Dupont, E., Cieniewski-Bernard, C., Bastide, B. & Stevens, L. 2011. Electrostimulation
568 during hindlimb unloading modulates PI3K-AKT downstream targets without
569 preventing soleus atrophy and restores slow phenotype through ERK. *American*
570 *Journal of Physiology: Regulatory, Integrative and Comparative Physiology*, **300**,
571 R408-17.
- 572 Egawa, T., Ohno, Y., Goto, A., Ikuta, A., Suzuki, M., Ohira, T., Yokoyama, S., Sugiura, T.,
573 Ohira, Y., Yoshioka, T. & Goto, K. 2014. AICAR-induced activation of AMPK
574 negatively regulates myotube hypertrophy through the HSP72-mediated pathway in
575 C2C12 skeletal muscle cells. *Am J Physiol Endocrinol Metab*, **306**, E344-54.
- 576 Feng, Y., Huang, W., Meng, W., Jegga, A. G., Wang, Y., Cai, W., Kim, H. W., Pasha, Z., Wen,
577 Z., Rao, F., Modi, R. M., Yu, X. & Ashraf, M. 2014. Heat shock improves Sca-1+
578 stem cell survival and directs ischemic cardiomyocytes toward a prosurvival
579 phenotype via exosomal transfer: a critical role for HSF1/miR-34a/HSP70 pathway.
580 *Stem Cells*, **32**, 462-72.
- 581 Fitts, R. H., Metzger, J. M., Riley, D. A. & Unsworth, B. R. 1986. Models of disuse: a
582 comparison of hindlimb suspension and immobilization. *J Appl Physiol* **60**, 1946-53.
- 583 Gan, Z., Rumsey, J., Hazen, B. C., Lai, L., Leone, T. C., Vega, R. B., Xie, H., Conley, K. E.,
584 Auwerx, J., Smith, S. R., Olson, E. N., Kralli, A. & Kelly, D. P. 2013. Nuclear
585 receptor/microRNA circuitry links muscle fiber type to energy metabolism. *J Clin*

- 586 *Invest*, **123**, 2564-75.
- 587 Glass, D. J. 2003. Molecular mechanisms modulating muscle mass. *Trends in Molecular*
- 588 *Medicine*, **9**, 344-50.
- 589 Haddad, F., Qin, A. X., Zeng, M., McCue, S. A. & Baldwin, K. M. 1998. Interaction of
- 590 hyperthyroidism and hindlimb suspension on skeletal myosin heavy chain expression.
- 591 *J Appl Physiol* **85**, 2227-36.
- 592 Hayashida, N., Fujimoto, M., Tan, K., Prakasam, R., Shinkawa, T., Li, L., Ichikawa, H.,
- 593 Takii, R. & Nakai, A. 2010. Heat shock factor 1 ameliorates proteotoxicity in
- 594 cooperation with the transcription factor NFAT. *EMBO J*, **29**, 3459-69.
- 595 Hunter, R. B. & Kandarian, S. C. 2004. Disruption of either the Nfkb1 or the Bcl3 gene
- 596 inhibits skeletal muscle atrophy. *Journal of Clinical Investigation*, **114**, 1504-11.
- 597 Inouye, S., Izu, H., Takaki, E., Suzuki, H., Shirai, M., Yokota, Y., Ichikawa, H., Fujimoto, M.
- 598 & Nakai, A. 2004. Impaired IgG production in mice deficient for heat shock
- 599 transcription factor 1. *J Biol Chem*, **279**, 38701-9.
- 600 Jiang, H., Li, H. & DiMario, J. X. 2006. Control of slow myosin heavy chain 2 gene
- 601 expression by glycogen synthase kinase activity in skeletal muscle fibers. *Cell Tissue*
- 602 *Res*, **323**, 489-94.
- 603 Kamei, Y., Miura, S., Suzuki, M., Kai, Y., Mizukami, J., Taniguchi, T., Mochida, K., Hata, T.,
- 604 Matsuda, J., Aburatani, H., Nishino, I. & Ezaki, O. 2004. Skeletal muscle FOXO1

605 (FKHR) transgenic mice have less skeletal muscle mass, down-regulated Type I
 606 (slow twitch/red muscle) fiber genes, and impaired glycemic control. *Journal of*
 607 *Biological Chemistry*, **279**, 41114-23.

608 Koya, T., Nishizawa, S., Ohno, Y., Goto, A., Ikuta, A., Suzuki, M., Ohira, T., Egawa, T.,
 609 Nakai, A., Sugiura, T., Ohira, Y., Yoshioka, T., Beppu, M. & Goto, K. 2013. Heat
 610 shock transcription factor 1-deficiency attenuates overloading-associated hypertrophy
 611 of mouse soleus muscle. *PLoS One*, **8**, e77788.

612 Kubis, H. P., Scheibe, R. J., Meissner, J. D., Hornung, G. & Gros, G. 2002. Fast-to-slow
 613 transformation and nuclear import/export kinetics of the transcription factor NFATc1
 614 during electrostimulation of rabbit muscle cells in culture. *J Physiol*, **541**, 835-47.

615 Li, Y., Xu, D., Bao, C., Zhang, Y., Chen, D., Zhao, F., Ding, J., Liang, L., Wang, Q., Liu, L.,
 616 Li, J., Yao, M., Huang, S. & He, X. 2014. MicroRNA-135b, a HSF1 target, promotes
 617 tumor invasion and metastasis by regulating RECK and EVI5 in hepatocellular
 618 carcinoma. *Oncotarget*.

619 Lindquist, S. 1986. The heat-shock response. *Annu Rev Biochem*, **55**, 1151-91.

620 Lodka, D., Pahuja, A., Geers-Knörr, C., Scheibe, R., Nowak, M., Hamati, J., Köhncke, C.,
 621 Purfürst, B., Kanashova, T., Schmidt, S., Glass, D. J., Morano, I., Heuser, A., Kraft,
 622 T., Bassel-Duby, R., Olson, E. N., *et al.* 2015. Muscle RING-finger 2 and 3 maintain
 623 striated-muscle structure and function. *Journal of Cachexia, Sarcopenia and Muscle*.

- 624 McCarthy, J. J., Esser, K. A., Peterson, C. A. & Dupont-Versteegden, E. E. 2009. Evidence
625 of MyomiR network regulation of beta-myosin heavy chain gene expression during
626 skeletal muscle atrophy. *Physiol Genomics*, **39**, 219-26.
- 627 Mitchell, P. O. & Pavlath, G. K. 2001. A muscle precursor cell-dependent pathway
628 contributes to muscle growth after atrophy. *American Journal of Physiology: Cell
629 Physiology*, **281**, C1706-15.
- 630 Naya, F. J., Mercer, B., Shelton, J., Richardson, J. A., Williams, R. S. & Olson, E. N. 2000.
631 Stimulation of slow skeletal muscle fiber gene expression by calcineurin in vivo. *J
632 Biol Chem*, **275**, 4545-8.
- 633 Neal, J. W. & Clipstone, N. A. 2001. Glycogen synthase kinase-3 inhibits the DNA binding
634 activity of NFATc. *J Biol Chem*, **276**, 3666-73.
- 635 Nishizawa, S., Koya, T., Ohno, Y., Goto, A., Ikuita, A., Suzuki, M., Ohira, T., Egawa, T.,
636 Nakai, A., Sugiura, T., Ohira, Y., Yoshioka, T., Beppu, M. & Goto, K. 2013.
637 Regeneration of injured skeletal muscle in heat shock transcription factor 1-null mice.
638 *Physiol Rep*, **1**, e00071.
- 639 Ohira, Y., Yoshinaga, T., Ohara, M., Kawano, F., Wang, X. D., Higo, Y., Terada, M.,
640 Matsuoka, Y., Roy, R. R. & Edgerton, V. R. 2006. The role of neural and mechanical
641 influences in maintaining normal fast and slow muscle properties. *Cells Tissues
642 Organs*, **182**, 129-42.

- 643 Oishi, Y., Ogata, T., Yamamoto, K. I., Terada, M., Ohira, T., Ohira, Y., Taniguchi, K. & Roy,
 644 R. R. 2008. Cellular adaptations in soleus muscle during recovery after hindlimb
 645 unloading. *Acta Physiol (Oxf)*, **192**, 381-95.
- 646 Rao, A., Luo, C. & Hogan, P. G. 1997. Transcription factors of the NFAT family: regulation
 647 and function. *Annu Rev Immunol*, **15**, 707-47.
- 648 Reilly, M. E., McKoy, G., Mantle, D., Peters, T. J., Goldspink, G. & Preedy, V. R. 2000.
 649 Protein and mRNA levels of the myosin heavy chain isoforms I β , IIa, IIx and IIb
 650 in type I and type II fibre-predominant rat skeletal muscles in response to chronic
 651 alcohol feeding. *Journal of Muscle Research and Cell Motility*, **21**, 763-73.
- 652 Sandona, D., Desaphy, J. F., Camerino, G. M., Bianchini, E., Ciciliot, S., Danieli-Betto, D.,
 653 Dobrowolny, G., Furlan, S., Germinario, E., Goto, K., Gutschmann, M., Kawano, F.,
 654 Nakai, N., Ohira, T., Ohno, Y., Picard, A., *et al.* 2012. Adaptation of mouse skeletal
 655 muscle to long-term microgravity in the MDS mission. *PLoS One*, **7**, e33232.
- 656 Sandri, M., Sandri, C., Gilbert, A., Skurk, C., Calabria, E., Picard, A., Walsh, K., Schiaffino,
 657 S., Lecker, S. H. & Goldberg, A. L. 2004. Foxo transcription factors induce the
 658 atrophy-related ubiquitin ligase atrogin-1 and cause skeletal muscle atrophy. *Cell*,
 659 **117**, 399-412.
- 660 Shen, T., Cseresnyes, Z., Liu, Y., Randall, W. R. & Schneider, M. F. 2007. Regulation of the
 661 nuclear export of the transcription factor NFATc1 by protein kinases after slow fibre

- 662 type electrical stimulation of adult mouse skeletal muscle fibres. *J Physiol*, **579**,
 663 535-51.
- 664 Sugiura, T., Abe, N., Nagano, M., Goto, K., Sakuma, K., Naito, H., Yoshioka, T. & Powers, S.
 665 K. 2005. Changes in PKB/Akt and calcineurin signaling during recovery in atrophied
 666 soleus muscle induced by unloading. *Am J Physiol Regul Integr Comp Physiol*, **288**,
 667 R1273-8.
- 668 Thomason, D. B. & Booth, F. W. 1990. Atrophy of the soleus muscle by hindlimb
 669 unweighting. *J Appl Physiol*, **68**, 1-12.
- 670 Thomason, D. B., Herrick, R. E., Surdyka, D. & Baldwin, K. M. 1987. Time course of soleus
 671 muscle myosin expression during hindlimb suspension and recovery. *J Appl Physiol*,
 672 **63**, 130-7.
- 673 Tothova, J., Blaauw, B., Pallafacchina, G., Rudolf, R., Argentini, C., Reggiani, C. &
 674 Schiaffino, S. 2006. NFATc1 nucleocytoplasmic shuttling is controlled by nerve
 675 activity in skeletal muscle. *Journal of Cell Science*, **119**, 1604-11.
- 676 van der Velden, J. L., Langen, R. C., Kelders, M. C., Willems, J., Wouters, E. F.,
 677 Janssen-Heininger, Y. M. & Schols, A. M. 2007. Myogenic differentiation during
 678 regrowth of atrophied skeletal muscle is associated with inactivation of GSK-3beta.
 679 *Am J Physiol Cell Physiol*, **292**, C1636-44.
- 680 van Rooij, E., Quiat, D., Johnson, B. A., Sutherland, L. B., Qi, X., Richardson, J. A., Kelm,

- 681 R. J., Jr. & Olson, E. N. 2009. A family of microRNAs encoded by myosin genes
682 governs myosin expression and muscle performance. *Dev Cell*, **17**, 662-73.
- 683 White, J. R., Confides, A. L., Moore-Reed, S., Hoch, J. M. & Dupont-Versteegden, E. E.
684 2015. Regrowth after skeletal muscle atrophy is impaired in aged rats, despite similar
685 responses in signaling pathways. *Exp Gerontol*, **64**, 17-32.
- 686 Wojtaszewski, J. F., Nielsen, P., Kiens, B. & Richter, E. A. 2001. Regulation of glycogen
687 synthase kinase-3 in human skeletal muscle: effects of food intake and bicycle
688 exercise. *Diabetes*, **50**, 265-9.
- 689 Woodgett, J. R., Tonks, N. K. & Cohen, P. 1982. Identification of a calmodulin-dependent
690 glycogen synthase kinase in rabbit skeletal muscle, distinct from phosphorylase
691 kinase. *FEBS Letters*, **148**, 5-11.
- 692 Yamaguchi, T., Omori, M., Tanaka, N. & Fukui, N. 2013. Distinct and additive effects of
693 sodium bicarbonate and continuous mild heat stress on fiber type shift via
694 calcineurin/NFAT pathway in human skeletal myoblasts. *Am J Physiol Cell Physiol*,
695 **305**, C323-33.
- 696 Yasuhara, K., Ohno, Y., Kojima, A., Uehara, K., Beppu, M., Sugiura, T., Fujimoto, M., Nakai,
697 A., Ohira, Y., Yoshioka, T. & Goto, K. 2011. Absence of heat shock transcription
698 factor 1 retards the regrowth of atrophied soleus muscle in mice. *J Appl Physiol*, **111**,
699 1142-9.
- 700

Legends of figures

Figure 1. Changes in body weight and soleus muscle wet weight in response to 2-week hindlimb suspension followed by ambulation recovery. HSF1^{+/+}: wild-type mice; HSF1^{-/-}: heat shock transcription factor 1 null mice; Relative muscle weight: the muscle weight relative to body weight; Pre: before hindlimb suspension; R0, R2, and R4: recovery 0, 2, and 4 weeks, respectively. interaction: strain x time. ns: not significant. Values are means \pm SEM; $n = 5$ /mouse strain at each time point.

Figure 2. Typical transverse cryosections of the midbelly region of soleus muscle stained by immunofluorescence (A). Changes in the relative population of fiber type expressing MyHC of soleus muscle in response to 2-week hindlimb suspension followed by 4-week ambulation recovery (B). 1: type I fiber, 2a: type IIa fiber, 2bx: type II and/ or type 2x fiber. *Scale bars* = 50 μ m. Values are means \pm SEM; $n = 5$ /mouse strain at each time point. *: $p < 0.05$. See Figure 1 for other abbreviations, statistics, and symbols.

Figure 3. Expressions of NFAT isoforms in soleus muscle in response to hindlimb suspension followed by ambulation recovery. Representative expression patterns of NFATc1, NFATc2, NFATc3, NFATc4, and internal control β -actin (A). Changes in the mean levels of NFATc1, c2, c3, and c4 (B). Values are expressed relative to the value before hindlimb

720 suspension in HSF1^{+/+} (1.0). Values are means \pm SEM; $n = 5$ /mouse strain at each time point.

721 *: $p < 0.05$. See Figure 1 for other abbreviations, statistics, and symbols.

722

723 Figure 4. GSK3 α and GSK3 β phosphorylation in soleus muscle in response to hindlimb

724 suspension followed by ambulation recovery. Representative expression patterns of

725 phosphorylated GSK3 α (p-GSK3 α), total GSK3 α , p-GSK3 β and total GSK3 β (A). Changes

726 in the mean phosphorylation level of GSK3 α and GSK3 β (B). Values are expressed relative

727 to the value before hindlimb suspension in HSF1^{+/+} (1.0). Values are means \pm SEM; $n =$

728 5/mouse strain at each time point. See Figure 1 for other abbreviations, statistics, and

729 symbols. *: $p < 0.05$.

730

731 Figure 5. Expressions of microRNAs (miR-208b and miR-499) in soleus muscle in response

732 to hindlimb suspension followed by ambulation recovery. Values are expressed relative to the

733 value before hindlimb suspension in HSF1^{+/+} (1.0). Values are means \pm SEM; $n = 5$ /mouse

734 strain at each time point. *: $p < 0.05$. See Figure 1 for other abbreviations, statistics, and

735 symbols.

736

737 Figure 6. Expressions of slow myosin heavy chain (MyHC) mRNAs (Myh7 and Myh7b) in

738 soleus muscle in response to hindlimb suspension followed by ambulation recovery. Values

739 are expressed relative to the value before hindlimb suspension in HSF1^{+/+} (1.0). Values are
740 means \pm SEM; $n = 5$ /mouse strain at each time point. *: $p < 0.05$. See Figure 1 for other
741 abbreviations, statistics, and symbols.

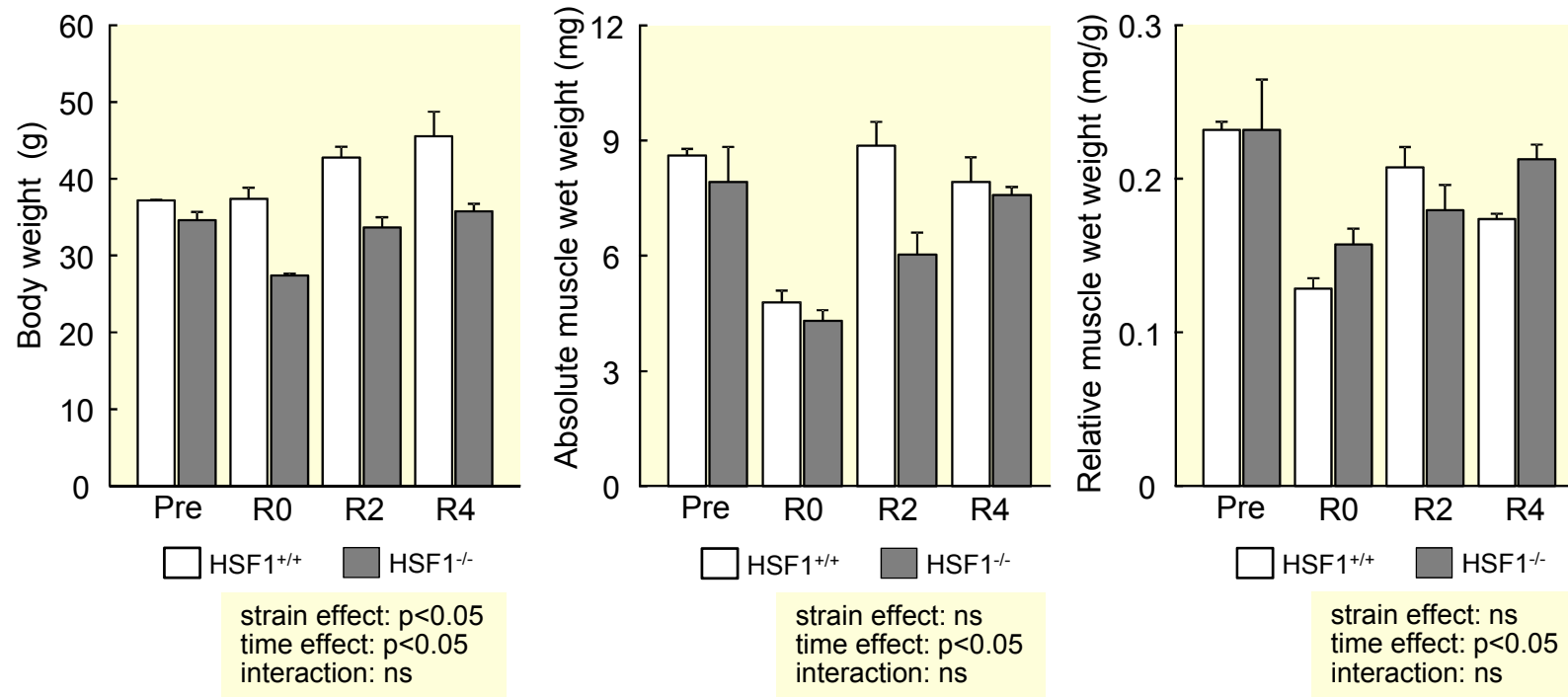


Figure 1

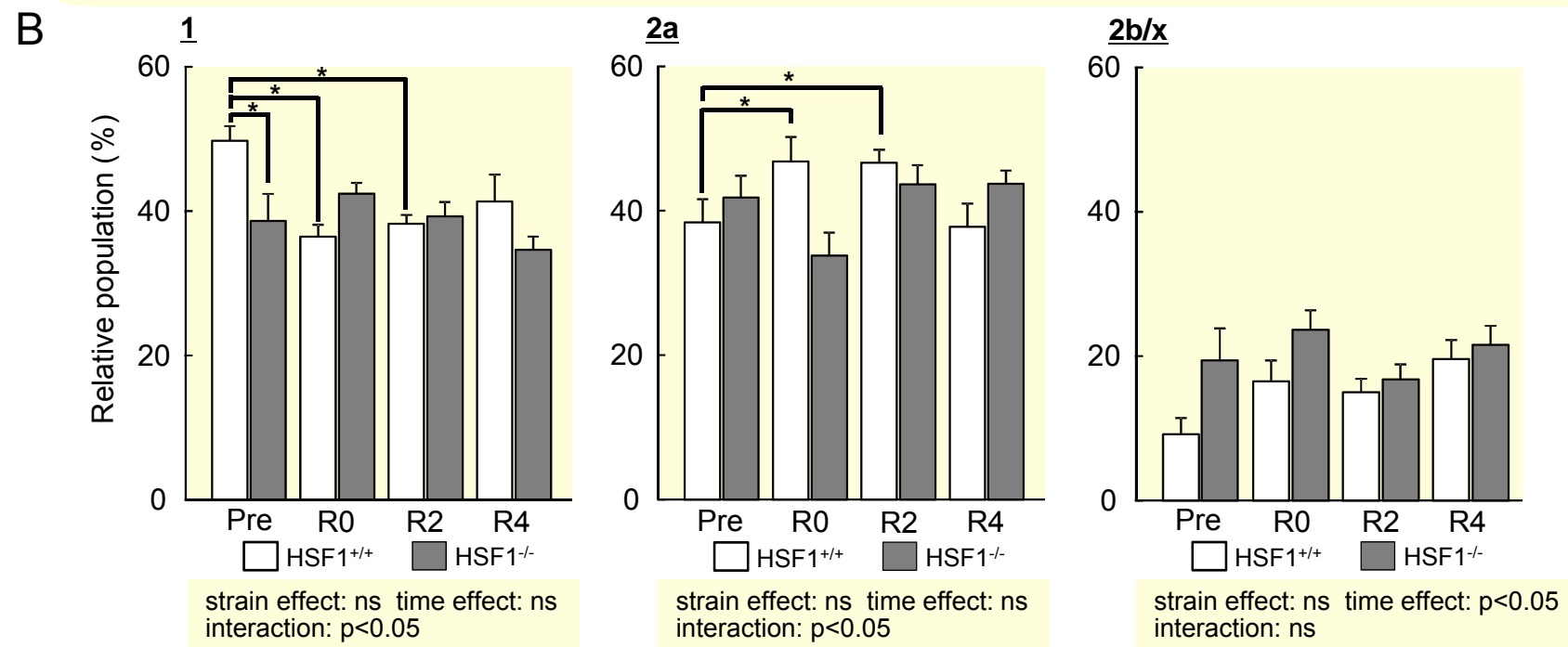
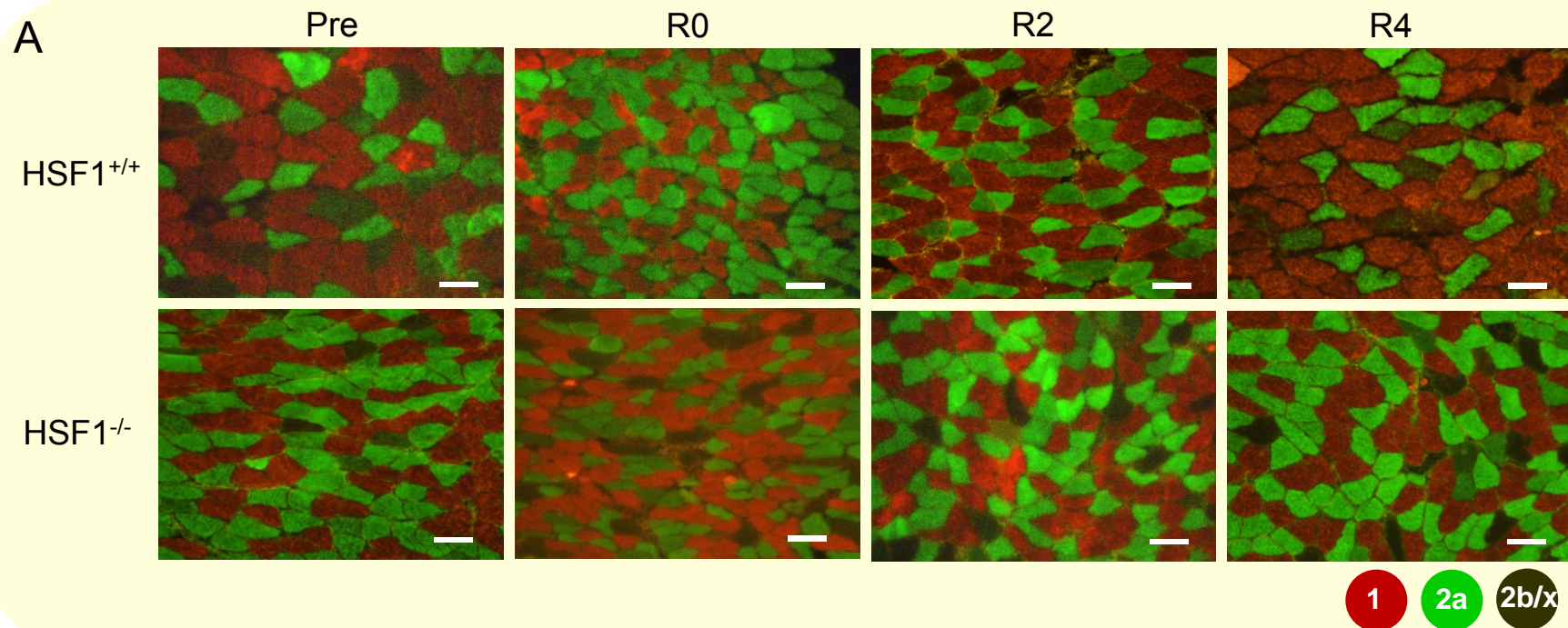


Figure 2

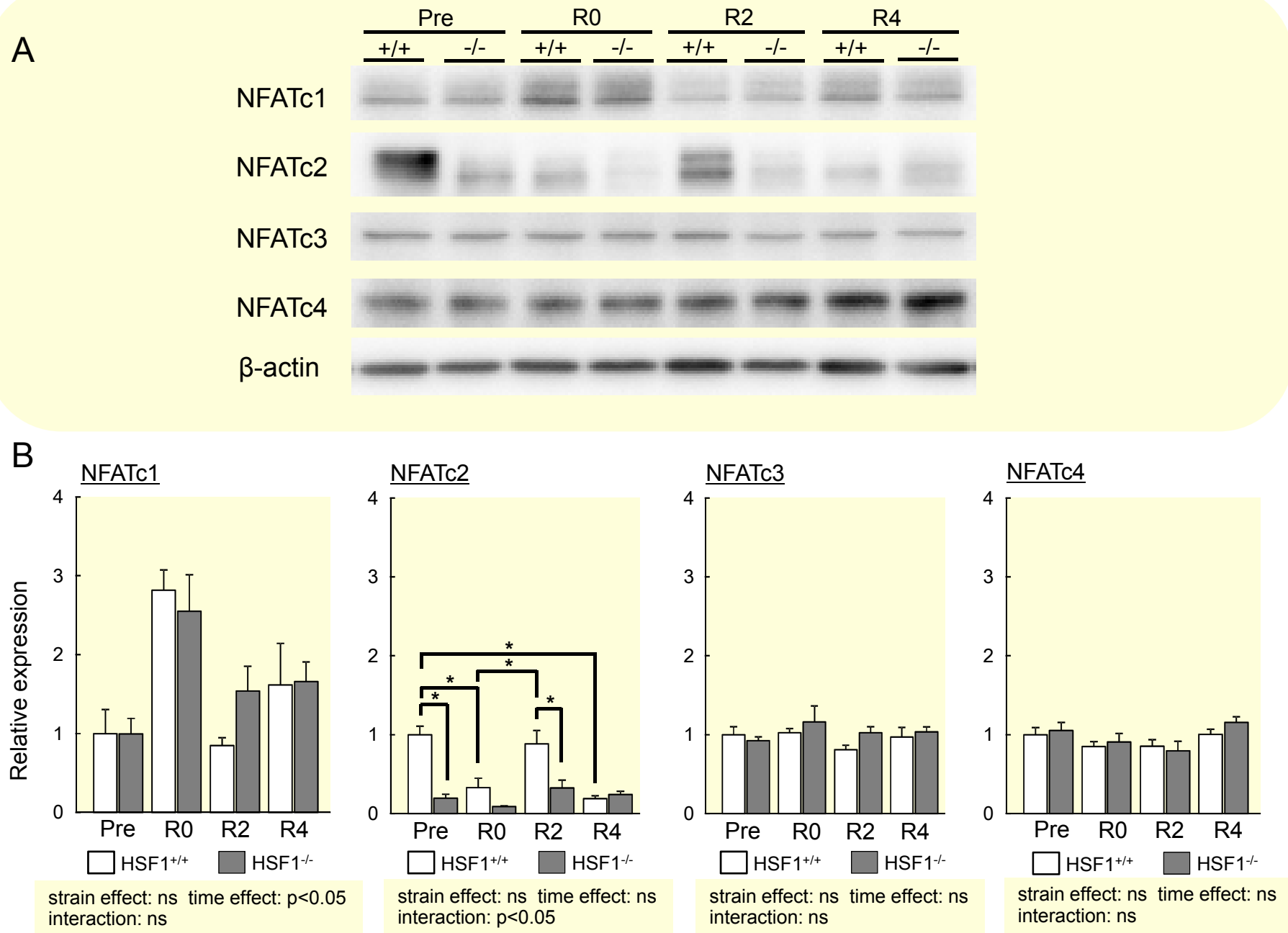


Figure 3

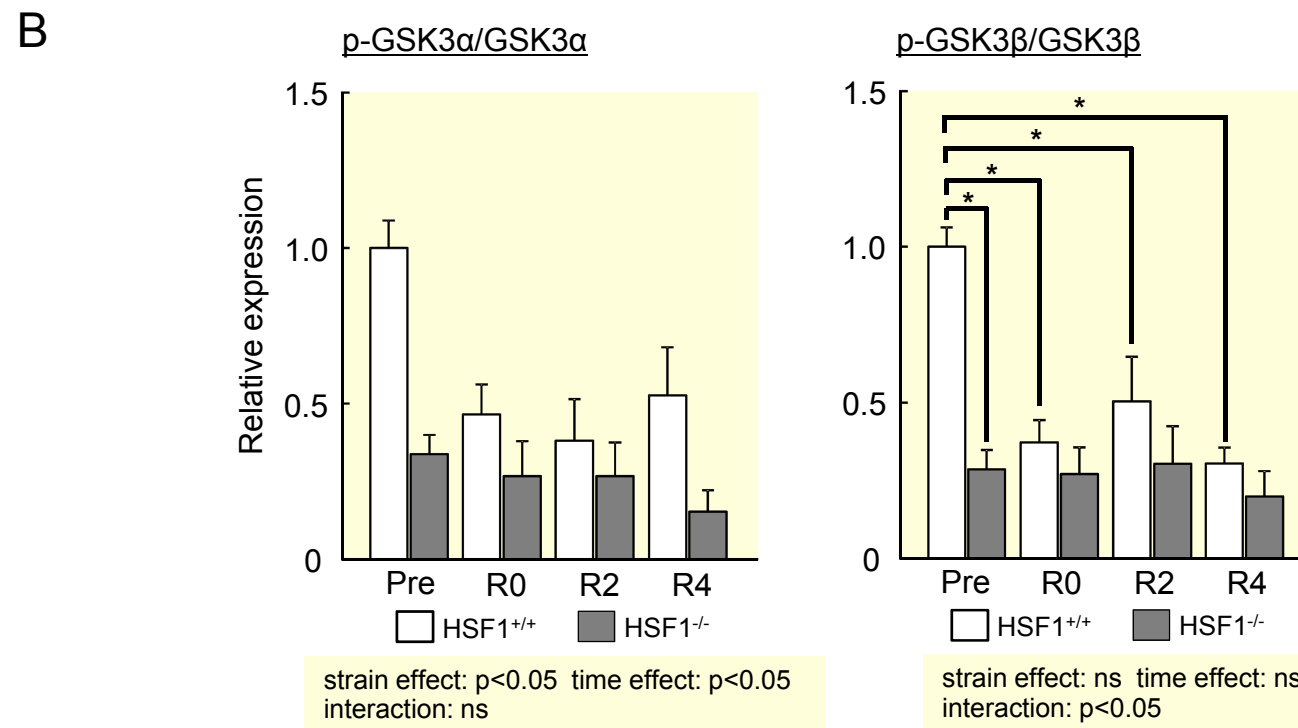
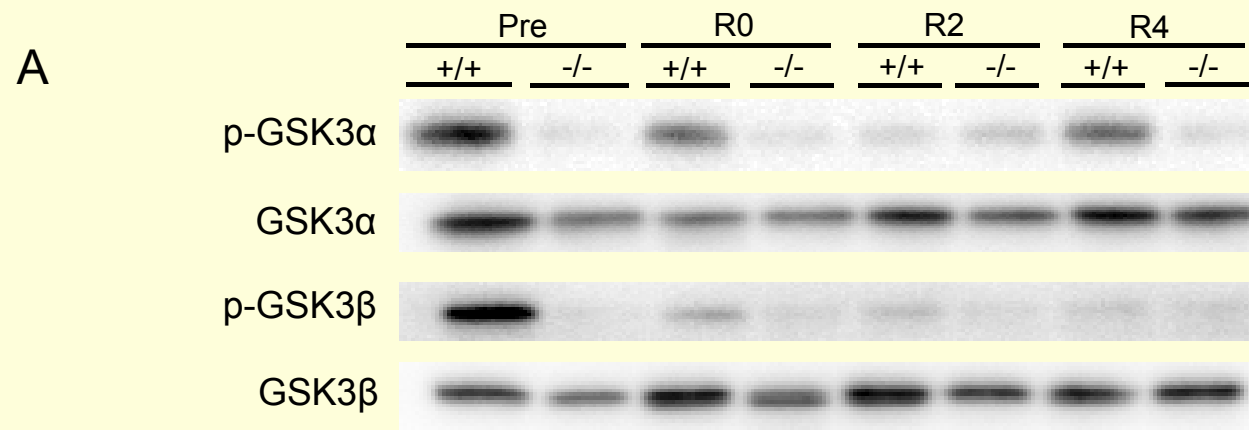


Figure 4

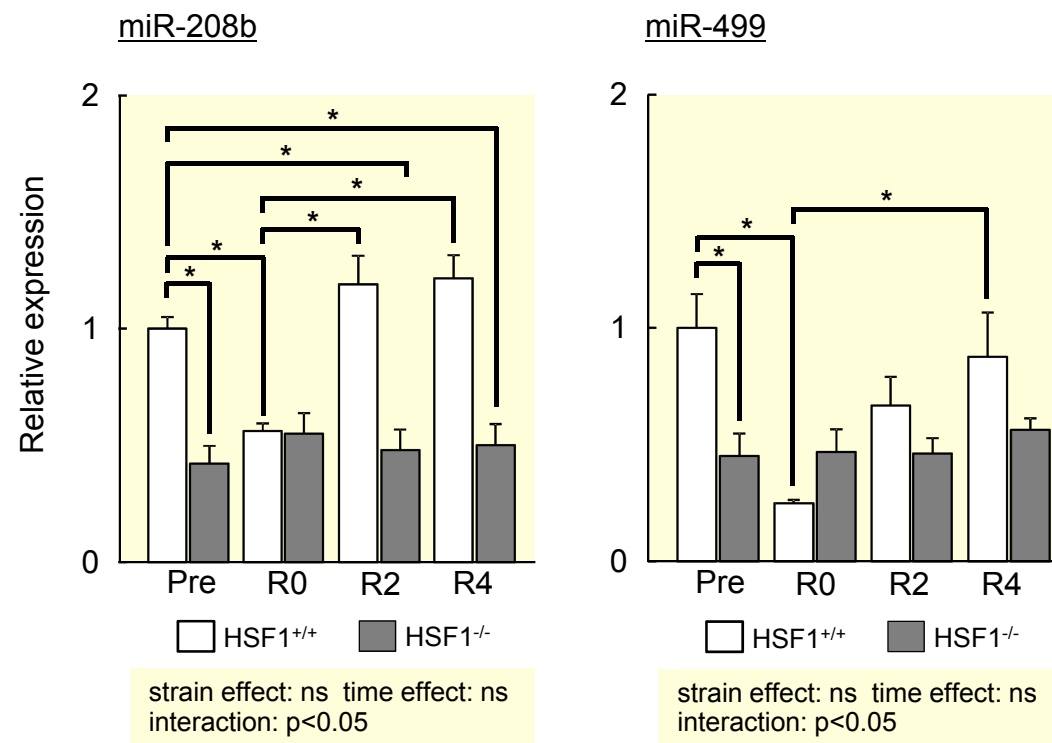


Figure 5

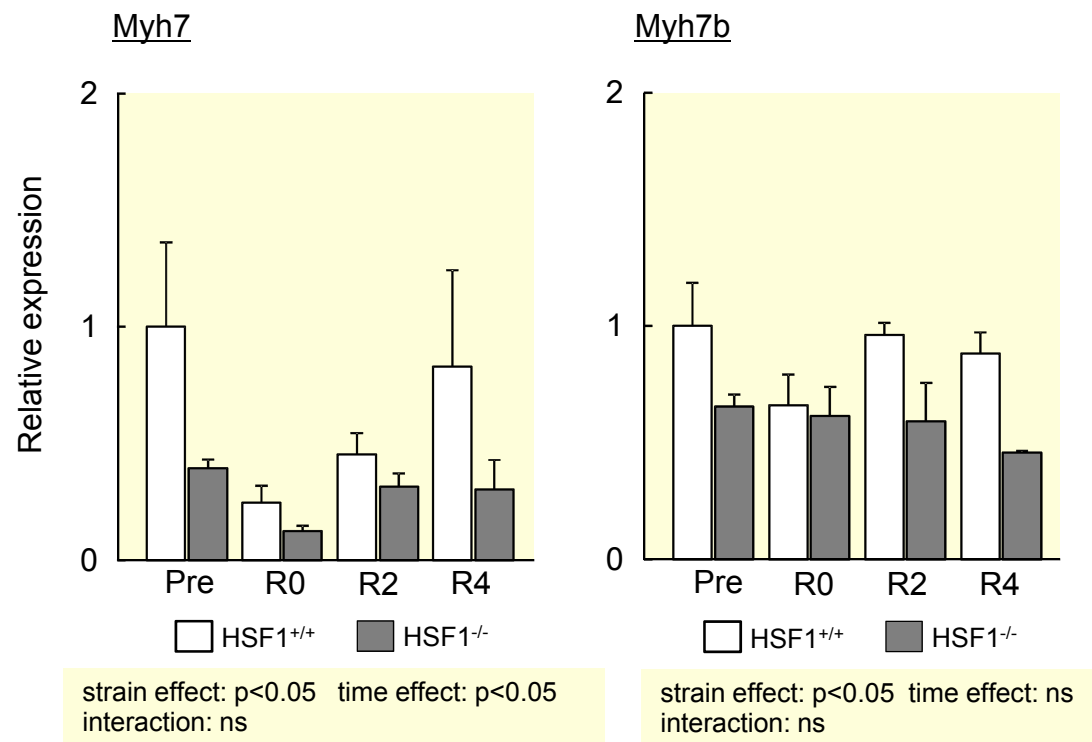


Figure 6